

## 温和条件下元素对 $M^{2+}/Fe^{2+}/Fe^{3+}$ -LDHs 转化成 尖晶石铁氧体过程的影响

董丽君 刘 耀 纪雪梅 魏亚波 徐庆红\*

(北京化工大学理学院, 化工资源有效利用国家重点实验室, 北京 100029)

**摘要:** 研究了二价金属离子在温和条件下(低于 100 °C, 暴露于空气中)从水滑石  $M^{2+}/Fe^{2+}/Fe^{3+}$ -LDHs( $M=Co, Ni, Mn, Zn$ )转化成尖晶石铁氧体的过程中所起的作用。结果表明, 该转化过程不仅与晶化温度有关, 还与  $M^{2+}$  在元素周期表中所处的位置有关。当这些二价金属离子处于同一周期并且相邻较近时,  $M^{2+}$  的半径越大, 水滑石微晶向尖晶石铁氧体的转化就越容易。此外,  $Fe^{2+}$  在转化过程中起着至关重要的作用, 如果没有  $Fe^{2+}$  的参与, 在此条件下的转化将无法进行。

**关键词:** 尖晶石铁氧体; 水滑石微晶; 转化; 元素影响; 温和条件

**中图分类号:** O614 **文献标识码:** A **文章编号:** 1001-4861(2014)05-1119-09

**DOI:** 10.11862/CJIC.2014.172

## Effect of Metal Ion on Conversion from $M^{2+}/Fe^{2+}/Fe^{3+}$ -LDHs to Spinel Ferrites under Mild Conditions

DONG Li-Jun LIU Yao JI Xue-Mei WEI Ya-Bo XU Qing-Hong\*

(State Key Laboratory of Chemical Resource Engineering, Beijing University of Chemical Technology,  
15 BeiSanhuan East Road, ChaoYang District, Beijing 100029, China)

**Abstract:** The Effect of divalent metal ion was studied on conversion of  $M^{2+}/Fe^{2+}/Fe^{3+}$ -LDHs ( $M=Co, Ni, Mn, Zn$ ) to spinel ferrites under mild conditions (below 100 °C in open air). The results show that the conversion is not only affected by aging temperature but also by position of  $M^{2+}$  in periodic table of elements. Large radius of  $M^{2+}$  ions will result in much easier formation of spinel ferrites from LDH microcrystallines when these ions are in the same period and close to each other. Also the existence of  $Fe^{2+}$  plays an important role in the process, and the conversion could not happen without participation of  $Fe^{2+}$  under the conditions studied.

**Key words:** spinel ferrite; LDH microcrystalline; conversion; elemental effects; mild conditions

### 0 Introduction

Spinel ferrite, a kind of soft magnetic material with formula of  $MFe_2O_4$  ( $M=Mn, Mg, Zn, Ni, Co$ , etc)<sup>[1-2]</sup>, has many interesting and important properties such as low melting point, high specific heating, large expansion coefficient, low saturation magnetic moment

and low magnetic transition temperature<sup>[3-5]</sup>. Owing to these properties, spinel ferrite has a wide application in microwave devices, radar, digital recording, catalysis, magnetic refrigeration systems, magnetic storage, ferro-fluid technology, and many bio-inspired applications (e.g. as drugs carriers for magnetically guided drug delivery and as contrast agents in magnetic

收稿日期: 2013-10-31。收修改稿日期: 2014-01-17。

国家自然科学基金(No.U1362113)、教育部科技创新基金的支持(No.pt2012112)资助项目。

\*通讯联系人。E-mail: xuqh@mail.buct.edu.cn, Tel: 010-64425037

resonance imaging)<sup>[6-12]</sup>. Metal cations have various combinations in the lattice of spinel ferrite, which are not only relative to the kind of metal cations but also to their physical and chemical environments. Performance of the material thus depends on its micro structural properties that are sensitive to its mode of preparation<sup>[13-15]</sup>.

Conventional chemical methods have been used to prepare nanocrystalline soft ferrite, which includes sol-gel<sup>[16]</sup>, coprecipitation<sup>[17-18]</sup>, solvothermal, combustion, etc<sup>[19]</sup>. But these methods have more or less disadvantages. Physical methods have many drawbacks such as requirement of sophisticated instruments, high cost, and wastage of material. Preparation of ferrites by conventional ceramic method will produce heterogeneous large particle size and low surface area materials<sup>[20]</sup>. Moreover, the above methods also result in pollution and unsafe situations: risks of explosion often exist in energetic-ball-milling, solid-state preparation, and hydrothermal methods; pollution is also unavoidable in coprecipitation and sol-gel preparation. Therefore, preparation of spinel ferrites under mild conditions is necessary.

LDHs are a kind of two dimensional nano-structured anionic clays whose structures can be described as containing brucite-like layers in which a fraction of divalent cations have been replaced isomorphously by trivalent cations<sup>[21]</sup>. Research results indicate that LDHs are potential precursors for preparation of spinel ferrites because they are often formed with mixtures of the same cations and have been shown to have an absence of long-range cation ordering<sup>[22-23]</sup>. Some kinds of spinel ferrites were prepared from 1999<sup>[24]</sup> to 2004<sup>[25]</sup> using the LDHs as precursors, but they were all synthesized under high temperatures.

In 2009,  $\text{MgFe}_2\text{O}_4$  was firstly prepared by conversion of  $\text{Mg}^{2+}/\text{Fe}^{2+}/\text{Fe}^{3+}$ -LDHs below 100 °C<sup>[26]</sup>. In this work,  $\text{M}^{2+}/\text{Fe}^{2+}/\text{Fe}^{3+}$ -LDHs ( $\text{M}=\text{Co}, \text{Ni}, \text{Mn}, \text{Zn}, \text{Mg/Co}$  and  $\text{Mg/Ni}$ ) were studied and their corresponding spinel ferrite nanoparticles were all prepared under 100 °C at one atmosphere pressure. It was found that the conversion process of LDHs was not only affected

by aging temperatures but also by existence of  $\text{Fe}^{2+}$ , especially affected strongly by the existence of divalent metallic ions with different activities. Some electrodes, formed between  $\text{M}^{2+}$  or  $\text{M}^{2+}/\text{M}'^{2+}$  to  $\text{Fe}^{2+}$  or  $\text{Fe}^{2+}/\text{Fe}^{3+}$ , were considered to be formed in the conversion process, and they affected the microcrystal conversions from  $\text{M}^{2+}/\text{Fe}^{2+}/\text{Fe}^{3+}$ -LDHs to spinel ferrites. PXRD patterns and SEM images prove the presence of spinel ferrite after  $\text{M}^{2+}/\text{Fe}^{2+}/\text{Fe}^{3+}$ -LDHs or their microcrystallines aged from 60 to 100 °C, and the results from characterizations on saturation magnetizations prove that the content of spinel ferrites is increased gradually with the aging temperature. Mössbauer spectroscopic analysis indicates that the elemental effect on the conversion of  $\text{M}^{2+}/\text{Fe}^{2+}/\text{Fe}^{3+}$ -LDHs to as-prepared spinel ferrite depends on the ratio of octahedral center site(A position) to tetrahedral center site (B position) when  $\text{M}^{2+}$  is different.

## 1 Experimental

### 1.1 Materials

Chemicals used were all of A.R. quality from Beijing Chemical Regent Company without further purification:  $\text{Fe}(\text{NO}_3)_3 \cdot 9\text{H}_2\text{O}$  (>98.5wt%);  $\text{FeSO}_4 \cdot 7\text{H}_2\text{O}$  (>99.0wt%);  $\text{Ni}(\text{NO}_3)_2 \cdot 6\text{H}_2\text{O}$  (>98.5wt%),  $\text{Co}(\text{NO}_3)_2 \cdot 6\text{H}_2\text{O}$  (>99.0wt%),  $\text{Mn}(\text{NO}_3)_2$  (solution in water, 50.0wt%),  $\text{Zn}(\text{NO}_3)_2 \cdot 6\text{H}_2\text{O}$  (>99.0wt%) and  $\text{Cu}(\text{NO}_3)$  (>99.0wt%).

Deionized water was used in all experiments.

### 1.2 Synthesis of $\text{M}^{2+}/\text{Fe}^{2+}/\text{Fe}^{3+}$ -LDHs and their spinel ferrites

Calculated amounts of  $\text{Co}(\text{NO}_3)_2 \cdot 6\text{H}_2\text{O}$ ,  $\text{Ni}(\text{NO}_3)_2 \cdot 6\text{H}_2\text{O}$ ,  $\text{Mn}(\text{NO}_3)_2$ ,  $\text{Zn}(\text{NO}_3)_2 \cdot 6\text{H}_2\text{O}$ ,  $\text{FeSO}_4 \cdot 7\text{H}_2\text{O}$ ,  $\text{Fe}(\text{NO}_3)_3 \cdot 9\text{H}_2\text{O}$  and  $\text{CuSO}_4 \cdot 5\text{H}_2\text{O}$  were dissolved in deionized and degassed water ( $C_{\text{M}^{2+}}$  and  $C_{\text{Fe}^{3+}}$  are all  $0.27 \text{ mol} \cdot \text{L}^{-1}$ ), respectively. Each solution above, about 100 mL, was adjusted to pH value about 10.5 with a mixed solution of  $\text{Na}_2\text{CO}_3$  and  $\text{NaOH}$  ( $C_{\text{NaOH}}=1.50 \text{ mol} \cdot \text{L}^{-1}$ ,  $C_{\text{Na}_2\text{CO}_3}=0.75 \text{ mol} \cdot \text{L}^{-1}$ ) to form suspensions, respectively. Each suspension was divided into four parts, and aged at different temperatures (from 40 °C to 100 °C) for 18~20 h in open air. The final products were obtained by centrifugation, washing with deionized and degassed water for several times, and drying at room temperature.

All processes were performed under the protection of nitrogen gas.

### 1.3 Characterization

X-ray diffraction (XRD) patterns were recorded on a Rigaku D/max-2500 diffractometer with a  $Cu K\alpha$  radiation ( $\lambda=0.15418\text{ nm}$ , scanning speed of  $10^\circ \cdot \text{min}^{-1}$ ) operated at 40 kV and 100 mA. Fourier transform infrared (FTIR) spectra were recorded in range of  $4000\sim400\text{ cm}^{-1}$  with  $2\text{ cm}^{-1}$  resolution on a Bruker Vector-22 Fourier transform spectrometer using KBr pellet technique (1.0 mg of sample in 100.0 mg of KBr). Thermogravimetry (TG) and differential scanning calorimetry (DSC) with  $\alpha\text{-Al}_2\text{O}_3$  as the reference were performed using HCT-2 thermoanalyzer (Beijing Hengjun Instrument Company) at a heating rate of  $10^\circ\text{C} \cdot \text{min}^{-1}$  from room temperature to  $580^\circ\text{C}$  in air. Magnetism of products was measured at room temperature on a JDM-13 vibration sample magnetometer. Scanning electronic microscopy (SEM) images of the

product were observed on a Shimadzu SS-550 microscope at 15 keV. Mössbauer spectra were recorded with an Oxford MS-500 instrument at 293 K, a radiation source of  $^{57}\text{Co}$  in an Rh matrix was used, and the isomer shifts were reported relative to sodium nitroprusside.

## 2 Results and discussion

SEM images of the products aged at 40, 60, 80 and  $100^\circ\text{C}$  are shown in Fig.1. Only particles with average diameter of  $30\sim40\text{ nm}$  are found in Mn-product, leaf-like with some plate-like morphology is found in Zn-product, only leaf-like morphology is found in Ni-product, and only plate-like morphology is found in Co-product after the four reactive mixtures are aged at  $40^\circ\text{C}$ . However after the mixtures are aged at  $60^\circ\text{C}$ , all plate-like morphology disappears but particles are found in Co-product, most of leaf-like morphology is disappeared and some particles

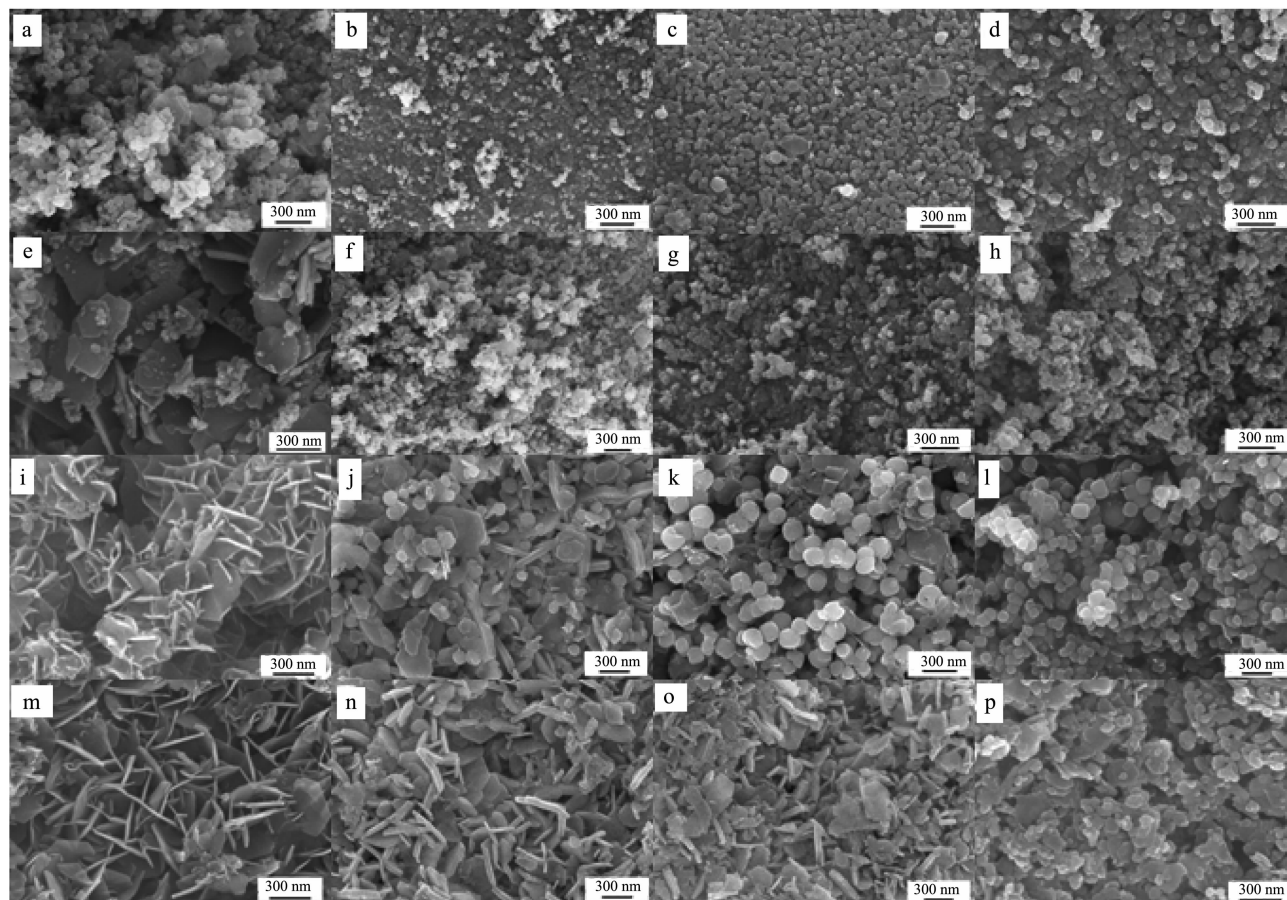


Fig.1 SEM images for the products aged at different temperatures: from a to d, e to h, i to l and m to p are Mn-, Co-, Zn- and Ni-products aged at 40, 60, 80 and  $100^\circ\text{C}$ , respectively



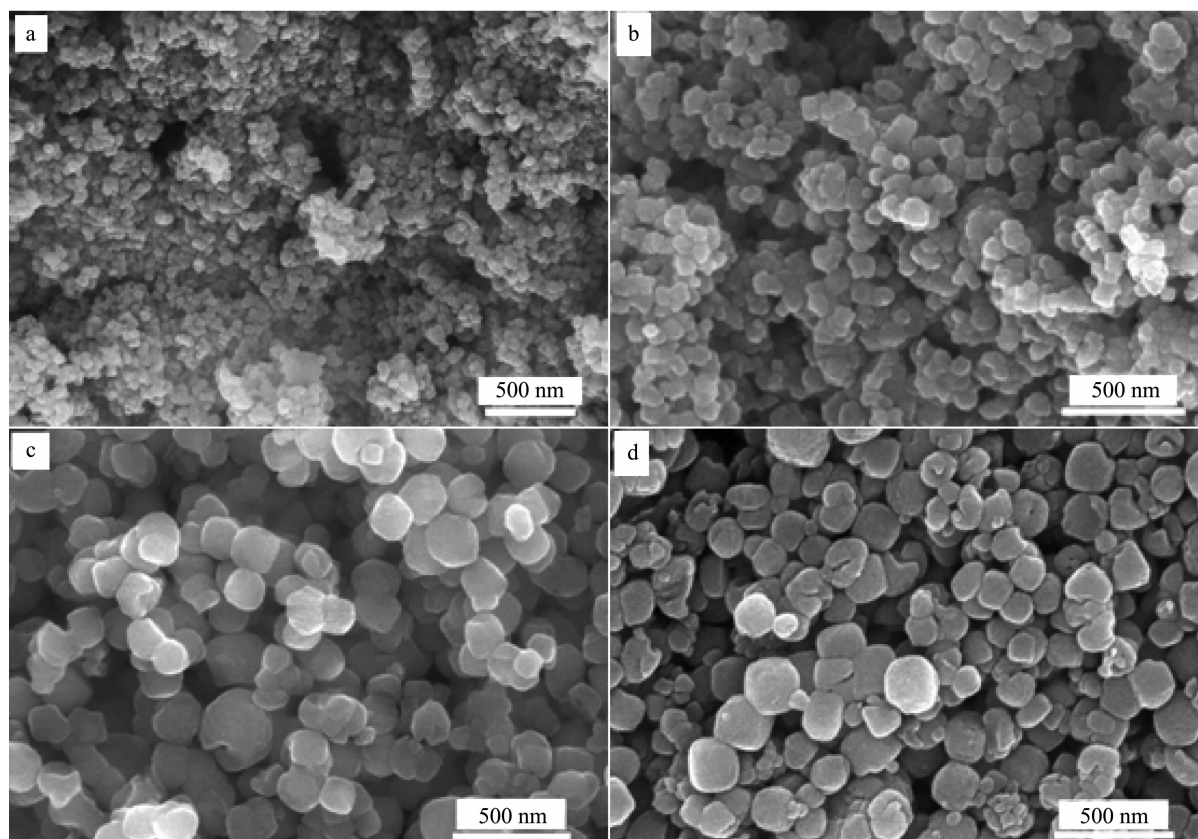


Fig.2 SEM images of aged products (at 100 °C) washed by HCl solution ( $C_{\text{HCl}}=12 \text{ mol} \cdot \text{L}^{-1}$ ):  
a, b, c and d are Mn-, Co-, Zn- and Ni-products, respectively

begin to appear in Zn-product (aging temperature for only particles in this product is about 80 °C). However in Ni-product, the leaf-like products could be still found until the aging temperature rises to 80 °C and the leaves are changed into some nanoparticles and plates after the sample is aged at 100 °C. The results indicate that the sequence of nanoparticles in the four aged products is different and the plate-like morphology possibly comes from the leaves disaggregated in aging course. An interesting phenomenon is found during the aging. Many small particles (possibly,  $\text{ZnCO}_3$ ,  $\text{CoCO}_3$  and  $\text{NiCO}_3$ ) are formed and adsorbed on the plates. After these products dissolve in HCl solution ( $C_{\text{HCl}}=12 \text{ mol} \cdot \text{L}^{-1}$ ), all plates are disaggregated to particles with a diameter of 80~100 nm (from Co-product), 150~180 nm (from Zn-product) and 150~200 nm (from Ni-product) (shown in Fig.2b, 2c and 2d). These nanoparticles are spinel ferrites as proved by PXRD characterization. So the formation sequence of spinel

ferrites with aging temperatures is Mn-product < Co-product < Zn-product < Ni-product, contrary to the radius sequence of  $\text{M}^{2+}$  ions.

PXRD patterns of these aged products are shown in Fig.3. Diffractions of the corresponding LDHs are found in Co-, Zn- and Ni-products under low aging temperatures. With the increased temperature, diffractions contributing to spinel ferrites (at about 31°, 35°, 43°, 53°, 57° and 63°) begin to appear in these products. In Co-product, diffractions from  $\text{Co}^{2+}\text{Fe}^{2+}\text{Fe}^{3+}$ -LDHs are very weak at 40 °C (Fig.3B), but diffractions from Co-spinel ferrite are found though they are very weak. After the aging temperature rises above 60 °C (inclusive of 60 °C), only diffractions of spinel ferrites are observed, indicating most of  $\text{Co}^{2+}\text{Fe}^{2+}\text{Fe}^{3+}$ -LDHs in this product are converted into spinel ferrites. To Zn-product, the aging temperature of 80 °C similar to Co-product is required, but diffraction peaks of  $\text{Ni}^{2+}\text{Fe}^{2+}\text{Fe}^{3+}$ -LDHs are still found clearly after they are aged at 100 °C. Contrary to the formers, seldom

diffractions from LDHs but spinel ferrites are found at any aging temperatures in Mn-product (Fig.3A), indicating Mn-spinel ferrite is the easiest formed in all the syntheses. As to Cu-system, no spinel ferrite and LDHs is formed at any aging temperatures (not listed). It possibly comes from the Ginger Taylor effect and the  $Cu^{2+}$  prefers to form planar coordination structure, which conflicts to the crystal structure of spinel ferrite and LDHs. In the figure, Aa, Bb, Cc and Dd are standard XRD patterns of the four spinel ferrites (coming from the software of MDI Jade5.0). It can be found that the spinel ferrites were really formed during the aging courses by comparisons. The yields of M-spinel ferrites at different aging temperatures are listed in Table 1.

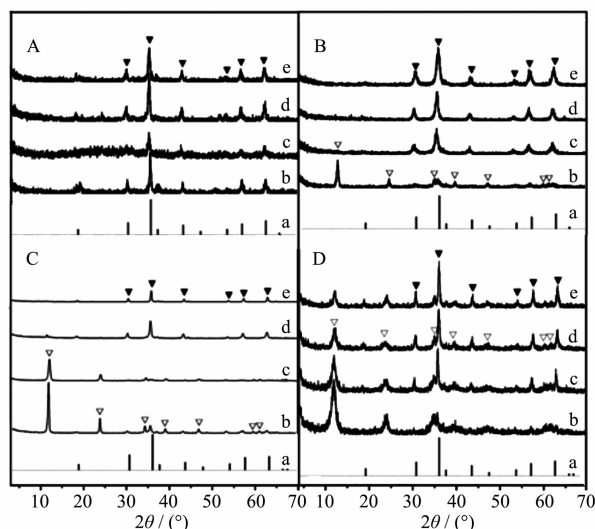


Fig.3 XRD patterns for standard spinel ferrites (a), the products aged at 40 °C (b), 60 °C (c), 80 °C (d) and 100 °C (e) for 20 h (▽ and ▼ are the characteristic diffractions of LDHs and spinel ferrite, respectively): A, B, C and D are Mn-, Co-, Zn- and Ni-samples, respectively

Also, during all experiments, there is no  $Fe_3O_4$  formed. The XRD diffractions of  $Fe_3O_4$  are at about

$30^\circ$ ,  $35^\circ$ ,  $42^\circ$  and  $62.5^\circ$ [27].

The above conversions are also reflected from their FTIR spectra (Fig.4). With increase of aging temperatures, bending vibrations of free  $CO_3^{2-}$  in interlayer of LDHs at  $1360\text{ cm}^{-1}$  are decreasing gradually in Co-, Zn- and Ni-products. To Co-product, absorption of  $CO_3^{2-}$  in  $Co^{2+}Fe^{2+}Fe^{3+}$ -LDHs disappears after the sample is aged at 60 °C and the phenomenon is also found in Zn-product after it is aged at 100 °C (absorptions of  $CO_3^{2-}$  from  $MCO_3$  are found on the left side of  $1360\text{ cm}^{-1}$  in the figure). However no absorption of  $CO_3^{2-}$  in interlayer of LDHs but in  $MnCO_3$  is found in Mn-product even the sample is aged at 40 °C, indicating no LDHs are formed in the synthesis, which is consistent with the results from XRD analysis. The absorptions of M-OHs, at about  $3375\text{ cm}^{-1}$ , in the structure of LDHs also show the same variable rules as those of  $CO_3^{2-}$  groups in interlayer.

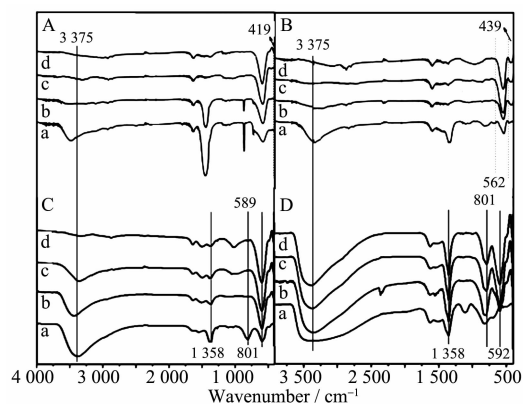


Fig.4 FTIR spectra of the products aged at 40 °C (a), 60 °C (b), 80 °C (c) and 100 °C (d): A, B, C and D are Mn-, Co-, Zn- and Ni-products, respectively

The change of infrared absorptions from  $Fe^{2+}$ -O and  $Fe^{3+}$ -O in these aged products also supports the above discussion. Stretching vibration absorptions of  $M^{2+}$ -O (M: Mn, Co, Zn and Ni) and  $Fe^{3+}$ -O bonds in tetrahedral and octahedral groups are known at about

Table 1 Conversion ratio of spinel ferrite in different reactive systems aged at different temperatures

M-spinel ferrite		Product aging temperature / °C			
		40	60	80	100
Conversion ratio / %	Mn	54.28	66.40	78.35	79.43
	Co	8.49	62.94	66.74	75.39
	Zn	4.73	38.07	54.06	57.90
	Ni	0.00	23.25	38.84	40.85

600  $\text{cm}^{-1}$  and 400  $\text{cm}^{-1}$  in spinel ferrites<sup>[28-29]</sup>, respectively. They are found at about 580~595  $\text{cm}^{-1}$  and 410~440  $\text{cm}^{-1}$  in some of our products in Fig.4. Before formation of the spinel ferrite, absorption of  $\text{Fe}^{2+}$  ions in LDHs is at about 800  $\text{cm}^{-1}$ <sup>[28]</sup>, which could be found in Co-, Zn- and Ni-products after they are aged at 40  $^{\circ}\text{C}$ . With increase of aging temperature, some LDHs disaggregate.  $\text{Fe}^{2+}$  ions are released from LDHs and oxidized to  $\text{Fe}^{3+}$  ions to enter into octahedral center, and  $\text{M}^{2+}$  ions are released from LDHs to enter tetrahedral center in spinel ferrites, the stretching vibration absorptions of  $\text{M}^{2+}\text{-O}$  and  $\text{Fe}^{3+}\text{-O}$  in spinel ferrites are enhanced, despite of the different enhanced speed in different aged products as shown

in Fig.4. However, absorption of  $\text{Fe}^{2+}\text{-O}$  in Mn-product is not found at any aging temperatures, indicating most of  $\text{Fe}^{2+}$  ions in the initial solution are oxidized and enters into framework of spinel ferrites directly. In Zn- and Co-products, absorption of  $\text{Fe}^{2+}\text{-O}$  in LDH (at about 793  $\text{cm}^{-1}$ ) is found at aging temperature of 40  $^{\circ}\text{C}$ , but it is hardly found after the sample is aged at 60  $^{\circ}\text{C}$ . Compared to Zn- and Co-products, decayed ratio of  $\text{Fe}^{2+}\text{-O}$  absorption in Ni-product is slower, it could be still found after the corresponding product is aged at 100  $^{\circ}\text{C}$ . Accompanying with the decrease of  $\text{Fe}^{2+}\text{-O}$  absorptions, absorptive intensity of  $\text{Fe}^{3+}\text{-O}$  (at about 400  $\text{cm}^{-1}$ ) in octahedral center of the aged products is increased gradually (Fig.4).

Table 2 Weight loss for four kinds of products aged at different temperatures

M-product		Product aging temperature / $^{\circ}\text{C}$			
		40	60	80	100
Weight loss / %	Mn	10.39	8.90	6.63	4.18
	Co	19.23	9.43	8.08	5.56
	Zn	31.52	12.31	5.76	2.71
	Ni	31.68	20.84	17.47	13.89

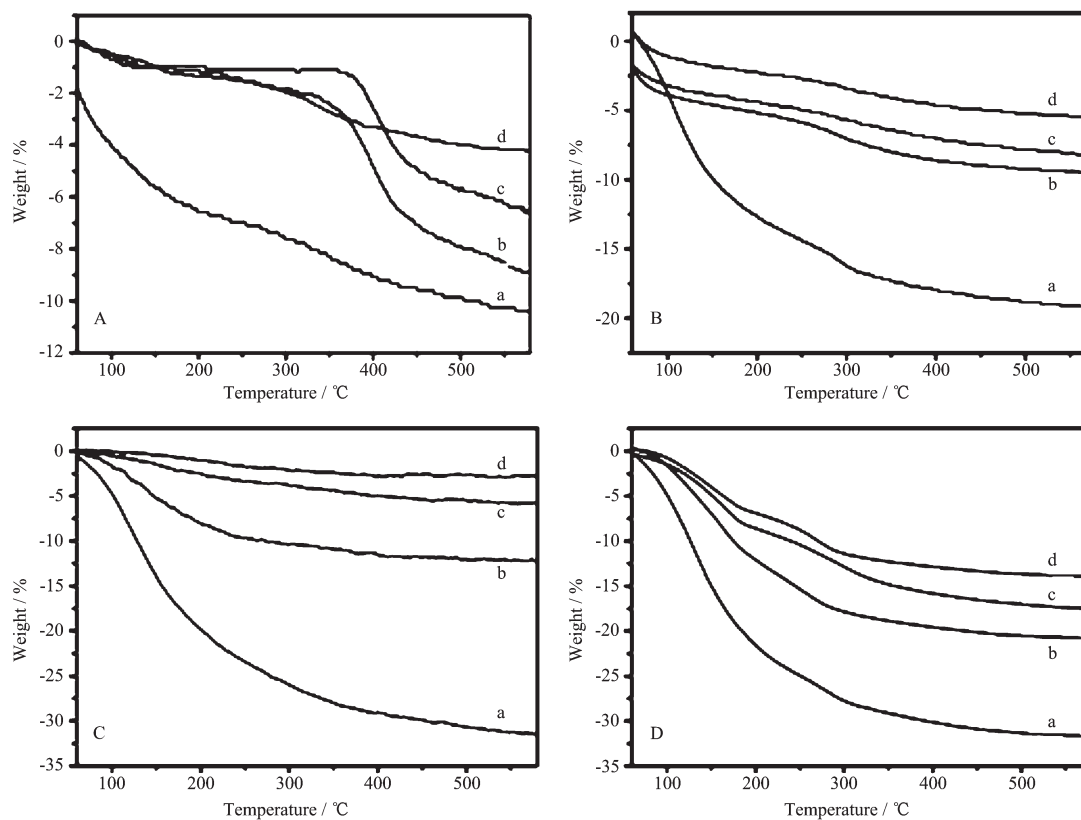


Fig.5 TG curves for the products aged at 40  $^{\circ}\text{C}$  (a), 60  $^{\circ}\text{C}$  (b), 80  $^{\circ}\text{C}$  (c) and 100  $^{\circ}\text{C}$  (d):

A, B, C and D are Mn-, Co-, Zn- and Ni-products, respectively

Elementary effect on conversion of  $M^{2+}/Fe^{2+}/Fe^{3+}$ -LDHs to spinel ferrites is also proved by TG analysis, and weight losses of the products aged at different temperatures are listed in Table 2 and shown in Fig.5. When aging temperature is at 40 °C, total weight loss of Zn- and Ni-products is almost the same, larger than that of Mn- and Co-products. Because most part of the products are LDHs and the weight loss comes from disaggregated  $CO_3^{2-}$  and water in interlayer and adsorbed on surface of LDHs. After the aging temperatures are raised above 60 °C and 80 °C, weight loss of Co- and Zn-products is getting less and less, because conversions from LDHs to spinel ferrites almost complete after the two products are aged at 60 °C and 80 °C, and weight loss of two products mainly comes from the adsorbed water and disaggregated  $MCO_3$ . Comparing to Co- and Zn-products, variations on weight loss of Ni-product aged at different temperatures are not so large, for their main component of LDHs. As to Mn-product, weight loss in every temperature step is less than the others, because of

almost no LDHs formation from initial aging temperature.

Mössbauer spectroscopic (assuming the ratio of recoilless fraction is  $f_B/f_A=0.94$  at room temperature) analyses indicate the elementary effects in as-prepared spinel ferrites by calculating change role of (A) position (octahedral center) and [B] position (tetrahedral center) when  $M^{2+}$  is different. As it is known that the fraction of (A) and [B] sites occupied by  $Fe^{3+}$  and  $M^{2+}$  in spinel ferrites, respectively,  $RA_{(A)[B]}$  will reflect the conversion course from LDHs to spinel ferrites, for (A) sites not only came from  $Fe^{3+}$  ions but also came from oxidized  $Fe^{2+}$  ions in conversions. Some values for  $RA_{(A)[B]}$  to different products aged at 60 °C were list in Table 3. The sequence of  $RA_{(A)[B]}$  in different products indicates that conversion in  $Co^{2+}/Fe^{2+}/Fe^{3+}$ -LDHs is the easiest and  $Ni^{2+}/Fe^{2+}/Fe^{3+}$ -LDHs

**Table 3**  $RA_{(A)[B]}$  calculated from mssbauer parameters in the products aged at 60 °C

	Mn-product	Co-product	Zn-product	Ni-product
$RA_{(A)[B]}$	1.29	1.25	0.73	0.61

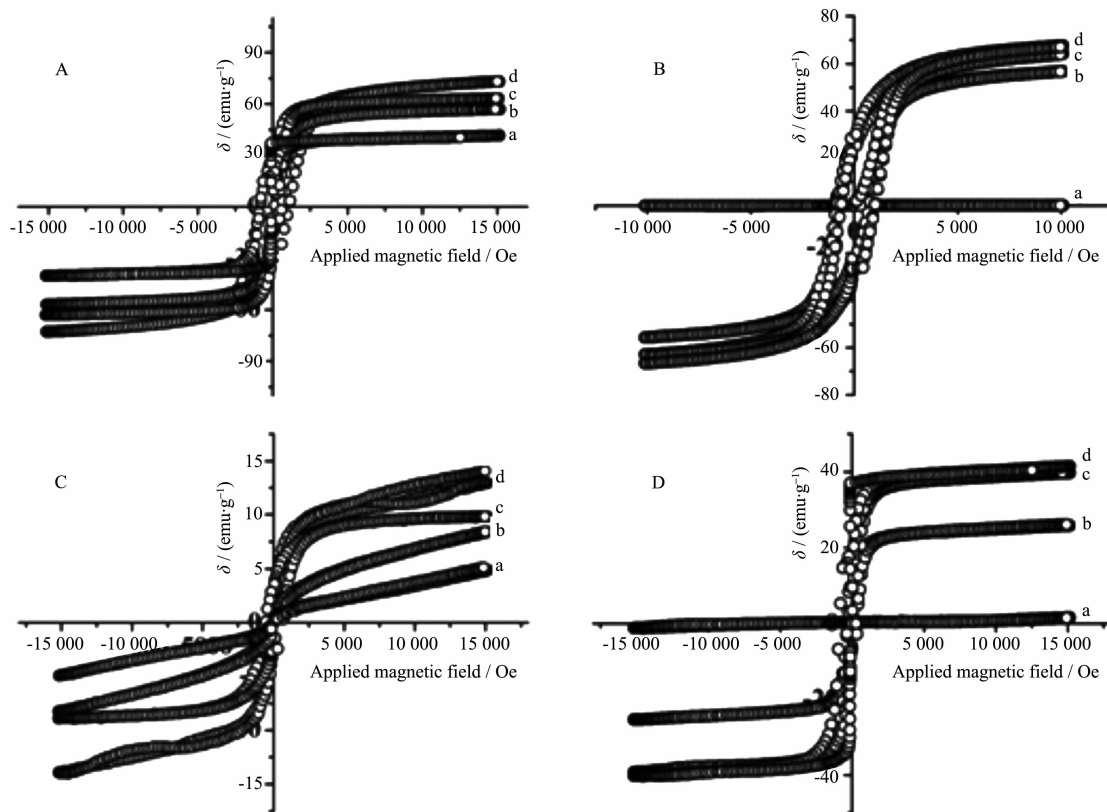


Fig.6 Hysteresis loops for products aged at 40 °C (a), 60 °C (b), 80 °C (c) and 100 °C (d):

A, B, C and D are Mn-, Co-, Zn- and Ni-products, respectively

**Table 4** Saturation magnetization values for four kinds of products aged at different temperatures

M-product		Product aged at temperature / °C			
		40	60	80	100
Saturation magnetization value / (emu·g <sup>-1</sup> )	Mn	38.81	53.29	60.18	69.11
	Co	3.12	50.87	59.69	61.45
	Zn	1.72	4.05	10.07	11.01
	Ni	1.40	23.56	37.19	38.71

is the most difficult. Hysteresis loops of four aged products at different temperatures were shown in Fig.6 and their corresponding saturation magnetization values were list in Table 4. The given results indicated that  $\delta$  (saturation magnetization) value of Mn-product is 38.81 emu·g<sup>-1</sup> and other products had almost no response in external magnetic field after aged at 40 °C. But when aging temperature was raised to 60 °C, all these products exhibit magnetic performances, and  $\delta$  values of Co-product is closed to that of the aged product at 100 °C. However, the required aging temperature is about 80 °C for Zn- and Ni-products.

The above results indicate that there exists a strong rule during formation of spinel ferrites in our work when M<sup>2+</sup> ions are different: Mn<sup>2+</sup> is easier than Co<sup>2+</sup>, Co<sup>2+</sup> is easier than Zn<sup>2+</sup>, Zn<sup>2+</sup> is easier than Ni<sup>2+</sup>, and Cu<sup>2+</sup> system cannot form spinel ferrites in synthesis. Considering they are in same period and sequence of their radius is Mn<sup>2+</sup>(0.080 nm) > Co<sup>2+</sup>(0.075 nm) > Zn<sup>2+</sup>(0.074 nm) > Ni<sup>2+</sup>(0.072 nm) > Cu<sup>2+</sup>(0.069 nm), formation of spinel ferrites (in Mn<sup>2+</sup> and Cu<sup>2+</sup> reactions) and conversion from LDHs to spinel ferrites (in Co<sup>2+</sup>, Zn<sup>2+</sup> and Ni<sup>2+</sup> reactions) are possibly contr-

olled by radius of M<sup>2+</sup> ions. Fig.7 shows some relationships between radii of M<sup>2+</sup> ions and the conversion ratios (%) from their corresponding LDHs to spinel ferrites. It can be clearly found that the yield of spinel ferrites decreases with radius decrease of M<sup>2+</sup> ions. The framework of LDHs are composed by M<sup>2+</sup>-O-Fe<sup>2+</sup> (Fe<sup>3+</sup>) (Scheme 1), bonds formation of M<sup>2+</sup>-O and O-Fe<sup>2+</sup>(Fe<sup>3+</sup>) will decide the yield of LDHs in different syntheses. Considering the scope of elements forming LDHs, smaller radius of M<sup>2+</sup> will be easy to enter centers of octahedral to form framework of LDHs accompanying Fe<sup>3+</sup> ions. But to M<sup>2+</sup> ions with large radius, it is difficult to form the framework of LDHs and the LDHs formed by this kind of ions will be not stable because of the crowded space around Fe<sup>3+</sup> ions. After these unstable LDHs are aged at a certain temperature, framework of the LDHs will be disaggregated and reassembly will happen. The disaggregation course will be easier with increase of M<sup>2+</sup> radius, and these disaggregated M<sup>n+</sup>-O (M: Fe<sup>3+</sup> and M<sup>2+</sup>) units in solution tend to form a more stable compound. In Fe<sup>3+</sup>-O units, Fe<sup>3+</sup> ions are in octahedral

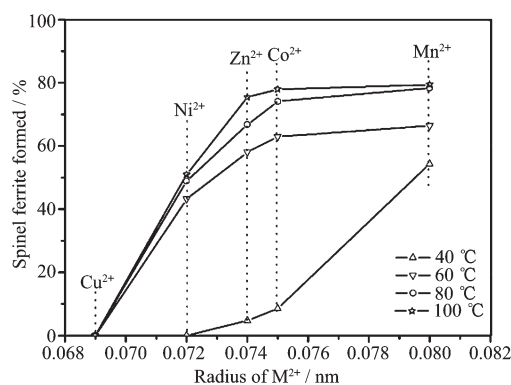
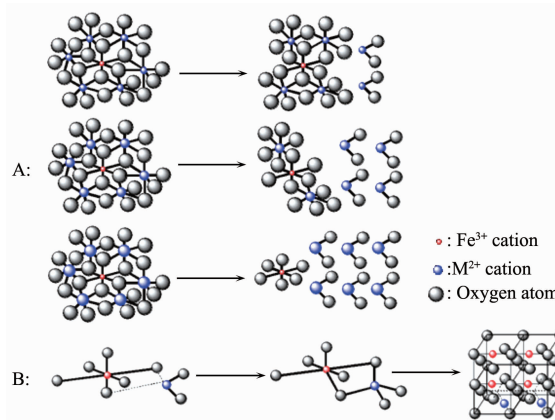


Fig.7 Relationships between radius of M<sup>2+</sup> ions and formation ratio of spinel ferrites (S. F.) (%) under different aging temperatures



Scheme 1 A: a simulative scheme on influence of M<sup>2+</sup> radii in disaggregated course of M<sup>2+</sup>/Fe<sup>2+</sup>/Fe<sup>3+</sup>-LDHs at a certain aging temperature; B: scheme for spinel ferrite's formation



center (hybridized orbital form of  $Fe^{3+}$  is  $d^2sp^3$ ) and  $M^{2+}$ -O units connecting to  $Fe^{3+}$  by oxygen are inclined to form tetrahedral center, which will decrease the space-block greatly. Spinel ferrites are then formed under this circumstance. A simulative course illustrating this conversion is shown in Scheme 1.

In addition, it should be mentioned that  $Fe^{2+}$  ions play an important role in conversion from  $M^{2+}/Fe^{2+}/Fe^{3+}$ -LDHs to their corresponding spinel ferrites. Without the participation of  $Fe^{2+}$ , the conversion could not happen. This issue is now under a further study.

### 3 Conclusions

Conversions from  $M^{2+}/Fe^{2+}/Fe^{3+}$ -LDHs ( $M=Co, Ni, Mn, Zn$ ) to spinel ferrites under 100 °C in open air were studied. The results show that the conversions are not only related to the aging temperature, but also to radius of  $M^{2+}$  ions.  $M^{2+}$  in  $M^{2+}/Fe^{2+}/Fe^{3+}$ -LDH with a small radius will lead to a difficult conversion to its corresponding spinel ferrite, and larger radius of  $M^{2+}$  in  $M^{2+}/Fe^{2+}/Fe^{3+}$ -LDHs will accelerate the conversion, i.e., there exist elementary matching effects in the LDHs when they are converted into spinel ferrites.  $Fe^{2+}$  ion plays an important role during the conversion, and conversion could not occur without the participation of  $Fe^{2+}$ .

**Acknowledgments:** We are grateful to the financial support from Project of National Natural Science Foundation of China (Project No.U1362113), the fund from Ministry of Education of China and the Program for Changjiang Scholars and Innovative Research Team in University (Project No. IRT0406).

### References:

- [1] Song Q, Zhang Z J. *J. Am. Chem. Soc.*, **2012**,**134**:10182-10190
- [2] Nejati K, Zabihi R. *Chem. Cent. J.*, **2012**,**23**:1-6
- [3] TIAN Ming-Bo (田民波). *Magnetic Materials* (磁性材料). Beijing: Tsinghua University Press, **2001**.
- [4] Widatallah H M, Al-Mamari F S A, Al-Saqri N A M, et al. *Mater. Chem. Phys.*, **2013**,**140**:97-103
- [5] Chen D, Zhang Y Z, Chen B Y, et al. *Ind. Eng. Chem. Res.*, **2013**,**52**:14179-14184
- [6] Puentes V F, Krishnan K M, Alivisatos A P. *Science*, **2001**, **291**:2115-2117
- [7] Lagarec K, Rancourt D G. *Recoil-Möbauer Spectral Analysis Software for Windows*, Version 1.02, Department of Physics, University of Ottawa, Ottawa, **1998**.
- [8] Gherca D, Comei N, Mentre O, et al. *Appl. Surf. Sci.*, **2013**, **10**:9-18
- [9] Yan K, Wu X, An X, Xie X M. *J. Alloys Compd.*, **2013**,**552**:405-408
- [10] Horvath M P. *J. Magn. Magn. Mater.*, **2000**,**215**:171-183
- [11] Adams J D, David L E, Dionne G F, et al. *Microwave Theory Tech.*, **2002**,**50**:721-737
- [12] Zhou Z H, Xue J M, Wang J. *J. Appl. Phys.*, **2002**,**91**:6015-6020
- [13] Yu S H, Yoshimura M. *Adv. Funct. Mater.*, **2002**,**12**:9-15
- [14] Pileni M P. *Adv. Funct. Mater.*, **2001**,**11**:323-331
- [15] Kulkarni R G, Joshi H H. *J. Solid State Chem.*, **1986**,**64**:141-147
- [16] Willey R J, Oliver S A, Oliveri G, et al. *Mater. Res.*, **1993**, **8**:1418-1427
- [17] Zhou J, Ma J F, Sun C, et al. *J. Am. Ceram. Soc.*, **2005**,**88**:3535-3537
- [18] Gheisari K, Shahriari S, Javadpour. *J. Alloys Compd.*, **2013**, **552**:146-151
- [19] Jiang J, Yang Y M, Li L C. *J. Alloys Compd.*, **2008**,**464**:370-373
- [20] Randhawa B S, Dosanjh H S, Kaur M. *J. Ceram. Inter.*, **2009**,**35**(3):1045-1049
- [21] (a) Rives V. *Layered Double Hydroxides: Present and Future*, New York: Nova Science Publishers, **2001**.  
(b) Cavani F, Trifiro F, Vaccari A. *Catal. Today*, **1991**,**11**:173-301
- [22] Vucelic M, Jones W, Moggridge G D. *Clays Clay Miner.*, **1997**,**45**:803-813
- [23] Iwasaki T, Shimizu K, Nakamura H, et al. *Mater. Lett.*, **2012**,**68**:406-408
- [24] Arco M D, Malet P, Trujillano R, et al. *Chem. Mater.*, **1999**, **11**:624-633
- [25] Li F, Liu J J, Evans D G, et al. *Chem. Mater.*, **2004**,**16**:1597-1602
- [26] Xu Q H, Wei Y B, Liu Y, et al. *Solid State Sci.*, **2009**,**11**:472-478
- [27] HUANG Jing-Jing (黄菁菁), XU Zu-Shun (徐祖顺), YI Chang-Feng (易昌凤). *J. Hubei Univ.* (湖北大学学报:自然科学版), **2007**,**29**(1):50-52
- [28] Sun G, Sun L, Wen H, et al. *J. Phys. Chem. B*, **2006**,**110**:13375-13380
- [29] Gotic M, Nagy I C, Popovic S, et al. *Magn. Lett.*, **1998**,**78**:193-201